Introduction

The joy and fun of understanding the universe we bequeath to our grandchildren -- and to their grandchildren. With over 90 percent of the matter in the universe still to play with, even the sky will not be the limit.

Vera Rubin

Every man dies, not every man really lives.

William Wallace
in movie Braveheart

Chapter 1

INTRODUCTION

In this thesis we describe various aspects of wide-field imaging with the Mauritius Radio Telescope (MRT). The hardware systems, the techniques and tools developed for wide-field imaging with the MRT and their application to the observations made are described. In this chapter we discuss, as a background to the thesis, some general aspects of surveying, aperture synthesis and protection of radio frequencies in astronomy .

1.1 Surveying

Surveying the sky and compiling catalogs of celestial objects has been a major part of astronomical research for centuries. The main idea behind surveying is to cover a large region and find out where things are. At high frequencies (i.e., frequencies greater than 1 GHz), surveying is an activity separate from that of high resolution imaging. It requires a different assessment of what is scientifically interesting and a different type of telescope. At low frequencies, however, there is no clear separation of these functions and so a high resolution telescope is also a surveying telescope [4].

The results of surveys are important for:

1. Selecting unbiased samples of objects from homogeneous catalogs for

further and more detailed studies.

2. Investigating catalogs to get cosmological information, e.g. clustering.

3. Surveys often lead to serendipitous discoveries or reveal new aspects of known objects. We give a few examples of such discoveries. Reber's 160 MHz maps showed that radio emission can also be non-thermal. The discovery of the microwave background was also serendipitous. Pulsars were discovered during a sky survey for scintillating sources. The first gravitationally lensed quasar appeared in the Jodrell Bank 960 MHz survey. BL Lac objects were recognized in early high frequency surveys and the first measurement of gravitational radiation came from a binary pulsar which was serendipitously found in a pulsar survey.

When one is thinking of doing a survey, some of the important questions that come up are [4]:

- What are the ultimate limits of resolution and sensitivity for the telescope?
- Given these constraints, what interesting science is possible ?
- How might the arrays be designed and built and where should they be located?

Surveys differ from each other in several respects [5]:

1. Frequency of observation.

   Measurements at different frequencies are used to establish the frequency dependence of emission. Specific frequencies are used for spectral-line

measurements which provide information about the composition and motion of the objects being studied.

2. Resolution of the survey telescope.

   High resolution is desirable because it can provide more detailed information about the structure of the object. At low frequencies, the resolution is also crucial in determining the depth of the survey, as most often, their sensitivity is limited by confusion noise.

3. Nature of the telescope employed in the survey.

   Each radio telescope has its own characteristic limitations. Many synthesis telescopes do not measure visibilities at short spacings[1].

4. Area of sky surveyed.

   Large catalogs are desirable for statistical work since the sampling error decreases as the size of the sample increases[2].

5. Sensitivity.

   Sensitivity determines the depth of the survey. At high frequencies, the limiting sensitivity is determined by the noise level of the telescope. At lower frequencies, the limit may be set by confusion.

6. Surveying sensitivity:

   Surveying sensitivity is the minimum flux density detectable in a survey of a particular region when the whole survey is completed in a total time t_s seconds. The sensitivity is expressed in terms of t_s rather than t, the time spent on the measurement in any one particular direction.

[1] The MRT measures visibilities down to zero-spacing and is sensitive to low surface-brightness objects and can detect very extended radio sources.

[2] The MRT in its final catalog is expected to have 10^5 sources.

7. Dynamic range of the images.

   Dynamic range is the ratio of the highest to the lowest brightness levels of reliable detail in the image.

The first systematic survey of the radio universe was carried out by Grote Reber **[6]** using a backyard telescope with a resolution of **12"** operating at a frequency of **160** MHz.

Freq.	Observatory	Resol.	Dec. Coverage	Sensit.	No. of Sources
Northern declination surveys					
408 MHz	Effelsberg	0.85° x 0.85"	$-10°to+50°$	0.2 Jv	–
178 MHz	Cambr. 3CR	2' x 2'	$-5°to+90"$	9 Jy	328
178 MHz	Cambr. 4C	7.5' x 7.5'	$-7°to+80"$	2 Jy	4843
38 MHz	Cambr. WKB	45' x 45'	$-45°to+35°$	14 Jy	1000
34.5 MHz	GEE TEE	30' x 30'	$-30°to+60°$	5 Jy	≈ 3000
151 MHz	Cambr. 6C	4' x 4'	$+30°to+90°$	0.12 Jy	$> 10^5$
Southern declination surveys					
38 MHz	Cambr. WKB	$45' \times 45'$	$-45°to+35°$	14 Jy	1000
34.5 MHz	GEE TEE	$30' \times 30'$	$-30°to+60°$	5 Jy	≈ 3000
408 MHz	Parkes	$0.85° \times 0.85°$	$-60°to+10°$	1 Jy	–
408 MHz	Molongolo	$2' \times 2'$	$-60°to+18°$	0.6 Jy	> 12000
843 MHz	MOST	$0.4' \times 0.4'$	$-90°to-30°$	–	ongoing
151.5 MHz	MRT	$4' \times 4'$	$-70°to-10°$	0.2 Jy	ongoing

Table **1.1:** Surveys below **1** GHz

With the quest for higher angular resolution, the exercise of surveying soon shifted to higher frequencies. Even so, many low frequency surveys were carried out after Reber's survey, some of which are summarized in Table **1.1.** The table clearly indicates that the sixth Cambridge survey (6C) [7] is by far the most extensive survey at low frequencies. This survey provided a moderately deep radio catalog reaching a source density of about 2×10^4 sr^{-1} over most of the sky north of declination (6) $+30°$ with an angular resolution of $4'.2 \times 4'.2$ $\mathrm{cosec}(\delta)$ and **a** limiting flux density of **120 mJy** at **151** MHz. An equivalent of the 6C survey for the southern sky, however, does not exist.

Since the survey of Mills et al. [8] at 80 MHz, there has not been much effort to map the southern sky at low frequencies, apart from the Parkes 408 MHz survey [9]. The Culgoora [10] observations at 80 and 160 MHz were made mainly to study known sources and to determine their spectral indices. The largest existing radio survey of the southern sky is the Parkes-MIT-NRAO survey [11] at 5 GHz.

A wide range of telescopes are being used to cover different parts of the spectrum and different parts of the sky, and many are either under construction or are being planned to fill in the gaps. Some of the recent, large continuum surveys or surveys underway, include the Westerbork Northern Sky Survey (WENSS), the VLA B-configuration Faint Images of the Radio Sky at Twenty Centimeters (FIRST) survey, NRAO VLA sky survey (NVSS), the MOST sky survey and the MRT sky survey discussed in this thesis. A new earth-based telescope, the Square Kilometer Array (SKA), is being planned with about a million square meter area. This is an international effort with various countries contributing towards its design and the selection of a suitable site.

There is a need to survey the southern sky at a frequency around 150 MHz. At this frequency synchrotron sources show up much better than at higher frequencies, such as 408 MHz, due to their spectra. Sources also show up better at 150 MHz than at lower frequencies since the absorption due to the interstellar gas is much less than at decameter wavelengths. For this purpose the Mauritius Radio Telescope (MRT) operating at $\sim$150 MHz has been built in Mauritius at a southern latitude of 20°.14 and eastern longitude of 57°.73. It is an aperture synthesis instrument and aims to survey the southern sky in the declination range $-70° \leq \delta \leq -10°$, covering the entire 24 hours of right ascension, with a resolution of 4' x 4'.6 $\sec(\delta + 20°.14)$ and a point source

sensitivity of $\sim$200 mJy (3σ) at 151.5 MHz.

Since the MRT is an aperture synthesis telescope we look at some basics of aperture synthesis in the next section.

1.2 Aperture synthesis

Aperture synthesis is an indirect imaging technique used in Radio Astronomy for obtaining high resolution images. The birth of aperture synthesis in radio astronomy[3] may be traced back to the pioneering paper in 1947 by McCready, Pawsey and Payne-Scott [12]. In this paper they said " ... It is possible in principle to determine the actual form of the distribution in a complex case by Fourier synthesis using information derived from a large number of components.". The first practical demonstration of one-dimensional aperture synthesis was done by Stanier at Cambridge in 1950 [13] on the radio observations of the Sun. O'Brien of Cambridge is credited for demonstrating the first two-dimensional aperture synthesis in 1953 [14] when he made partial use of the rotation of the Earth in doing a two-dimensional synthesis of the solar image. Ryle[4] and Neville in 1962 [15] performed a complete earth rotation synthesis for imaging the north polar region of the celestial sphere.

In aperture synthesis, instead of obtaining the image directly, Fourier components of the image, referred to as visibilities at different spatial frequencies, are measured from which the image is obtained through Fourier inversion (Van Cittert-Zernike theorem [16]).

The visibilities are measured using interferometers each formed by a pair of antennas. A simple 2-element interferometer is shown in Figure 1.1. The

[3] Historically the first application of aperture synthesis or indirect imaging, preceding radio astronomy by several decades, was in x-ray diffraction for crystallography.

[4] Martin Ryle received a Nobel Prize in 1974 for his contribution to aperture synthesis.

separation of the two antennas in the x, y plane is given by $D(x, \mathrm{y})$. The signals from the antennas pass through amplifiers which incorporate filters to select the required frequency bandwidth, Av, centered at a frequency ν_o.

The component in which the signals are combined is the correlator, which is a voltage multiplier followed by a time-averaging (integrating) circuit. The output of the correlator $\rho_D(x, \mathrm{y})$ is a measure of the visibility $V(x, \mathrm{y})$.

The relationship between the visibilities measured by the interferometers in the x, y plane (visibility plane) and the brightness distribution, B, in the ξ, η plane (image plane) may be written as follows:

$$\frac{A_N(\xi,\eta)B(\xi,\eta)}{\sqrt{1-\xi^2-\eta^2}} = \int\int V(x,y)e^{j2\pi(x\xi+y\eta)}\mathrm{d}x\mathrm{d}y \tag{1.1}$$

where x and y are in units of wavelength corresponding to the center frequency of received signals. In general, the brightness distribution of a radio source is real but not symmetric about any point and hence the visibility function, $V(x, \mathrm{y})$ (Fourier transform of brightness) is complex and hermitian symmetric.

$A_N(\xi, \eta)$ is the power pattern of an interferometer assumed to be identical for all the interferometers. This is in general equal to the product of the voltage patterns of the antennas forming the interferometer.

ξ is the direction cosine with respect to the x-axis. If the x-axis is defined along the east-west direction, then ξ is given by:

$$\xi = \cos\delta \sin \mathrm{H} \tag{1.2}$$

η is the direction cosine with respect to the y-axis. If the y-axis is defined

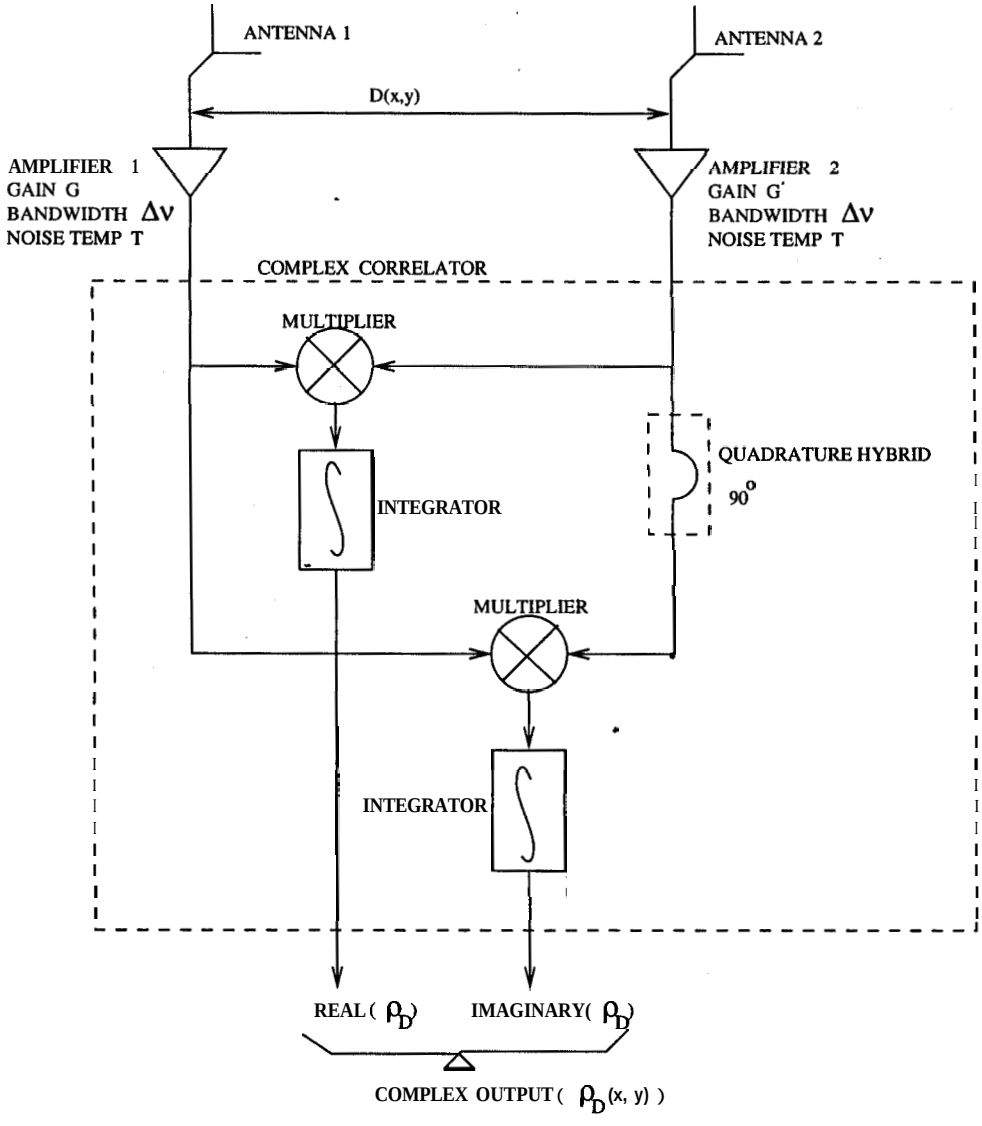

Figure 1.1: A simple block diagram of a two-element complex correlation interferometer

along the north-south direction, then η is given by:

$$\eta = \cos\delta \cos H \sin\phi - \sin\delta \cos\phi \tag{1.3}$$

where δ is the declination, H is the hour angle and ϕ is the latitude of the interferometer location.

In an array, if the antennas are not located in a plane, the visibilities measured are a function of x, y, and z, and Equation 1.1 may be written as:

$$\frac{A_N(\xi,\eta)B(\xi,\eta)}{\sqrt{1-\xi^2-\eta^2}} = \int\int\int V(x,y,z)e^{j2\pi(x\xi+y\eta+z\zeta)}\mathrm{d}x\mathrm{d}y\mathrm{d}z \tag{1.4}$$

where ζ is the direction cosine with respect to the z-axis. If the z-axis is defined along the zenith, then ζ is given by:

$$\zeta = \cos\delta \cos H \cos\phi + \sin\delta \sin\phi \tag{1.5}$$

ζ is related to the other two direction cosines by:

$$\zeta = \sqrt{1-\xi^2-\eta^2}$$

Therefore the relationship of the visibilities measured with a non-coplanar array and the sky brightness distribution may be written as:

$$\frac{A_N(\xi,\eta)B(\xi,\eta)}{\sqrt{1-\xi^2-\eta^2}} = \int\int\int V(x,y,z)e^{j2\pi\left(x\xi+y\eta+z\left(\sqrt{1-\xi^2-\eta^2}\right)\right)}\mathrm{d}x\mathrm{d}y\mathrm{d}z \tag{1.6}$$

Note that Equation 1.6 is not a three-dimensional Fourier transform relation between the visibility $V(x, \mathrm{y}, \mathrm{z})$ and the sky brightness $B(\xi,\eta)$. However, for computational purposes it may be convenient to use FFT. We therefore look at the relationship between the three-dimensional Fourier transform of $V(x, \mathrm{y}, z)$ known as the three-dimensional image volume, $F(\xi,\eta,\zeta)$ and the

two-dimensional sky brightness distribution $B(\xi,\eta)$. We follow Perley [17] in deriving the relationship.

Let $F(\xi,\eta,\zeta)$ be defined as the three-dimensional Fourier transform of the visibility function $V(x,\mathrm{y},\mathrm{x})$:

$$F(\xi,\eta,\zeta) = \int\int\int V(x,y,z)e^{j2\pi(x\xi+y\eta+z\zeta)}\mathrm{d}x\mathrm{d}y\mathrm{d}z \tag{1.7}$$

Now the measured visibility, $V(x,\mathrm{y},z)$, can be written as

$$V(x,y,z) = \int\int \frac{A_N(\xi,\eta)}{\sqrt{1-\xi^2-\eta^2}}B(\xi,\eta)e^{-j2\pi(x\xi+y\eta+z\sqrt{1-\xi^2-\eta^2})}\mathrm{d}\xi\mathrm{d}\eta \tag{1.8}$$

Substituting Equation 1.8 and using variables ξ' and η' to simplify the notation in Equation 1.7 gives:

$$F(\xi,\eta,\zeta) = \int\int\int \left\{ \int\int \frac{A_N(\xi',\eta')}{\sqrt{1-\xi'^2-\eta'^2}}B(\xi',\eta')e^{-j2\pi(x\xi'+y\eta'+z\sqrt{1-\xi'^2-\eta'^2})}\mathrm{d}\xi'\,\mathrm{d}\eta' \right\} e^{j2\pi(x\xi+y\eta+z\zeta)}\mathrm{d}x\mathrm{d}y\mathrm{d}z \tag{1.9}$$

The integrals over x, y, and x can be evaluated using the general result

$$\delta(\theta-\theta') = \int e^{-j2\pi x(\theta-\theta')}\mathrm{dx}$$

to get

$$F(\xi,\eta,\zeta) = \int\int \frac{A_N(\xi',\eta')}{\sqrt{1-\xi'^2-\eta'^2}}\delta(\xi'-\xi)\delta(\eta'-\eta)\delta(\sqrt{1-\xi'^2-\eta'^2}-\zeta)\mathrm{d}\xi'\mathrm{d}\eta' \tag{1.10}$$

Thus

$$F(\xi,\eta,\zeta) = \frac{A_N(\xi,\eta)B(\xi,\eta)\delta(\sqrt{1-\xi^2-\eta^2}-\zeta)}{\sqrt{1-\xi^2-\eta^2}} \tag{1.11}$$

The sky brightness distribution is a function of two variables, and the third variable ζ is introduced solely to establish a formal Fourier relation. The image volume $F(\xi,\eta,\zeta)$ is a function of three variables, but the only physically meaningful quantities within it lie on the sphere of unit radius defined by $\zeta = \sqrt{1-\xi^2-\eta^2}$.

Since, in practice, the visibilities are sampled at some discrete locations of the visibility function over a finite range, and could be measured with different weights, we introduce a weighting function $W(x,\mathrm{y},z)$ also known as the spectral sensitivity function or the transfer function with which the visibilities are multiplied. Therefore the image volume $\mathbf{F}(\xi,\eta,\zeta)$ gets convolved with $P(\xi,\eta,\zeta)$ which is the Fourier transform of $W(x,\mathrm{y},z)$

$$F(\xi,\eta,\zeta) = \frac{A_N(\xi,\eta)B(\xi,\eta)\delta(\sqrt{1-\xi^2-\eta^2}-\zeta)}{\sqrt{1-\xi^2-\eta^2}} \star\star\star P(\xi,\eta,\zeta) \tag{1.12}$$

where $\star\star\star$ represents a three dimensional convolution.

On the sphere where $\zeta = \sqrt{1-\xi^2-\eta^2}$, the brightness distribution $B_d(\xi,\eta)$ is:

$$B_d(\xi,\eta) = \frac{A_N(\xi,\eta)B(\xi,\eta)}{\sqrt{1-\xi^2-\eta^2}} \star\star P(\xi,\eta,\sqrt{1-\xi^2-\eta^2}) \tag{1.13}$$

Writing the convolution in terms of the integrals and substituting $B'(\xi,\eta)$ for $\frac{A_N(\xi,\eta)B(\xi,\eta)}{\sqrt{1-\xi^2-\eta^2}}$, we get

$$B_d(\xi,\eta) = \int\int B'(\xi,\eta)P(\xi'-\xi,\eta'-\eta,\sqrt{1-\xi'^2-\eta'^2}-\sqrt{1-\xi^2-\eta^2})\mathrm{d}\xi\mathrm{d}\eta \tag{1.14}$$

Let us consider an isolated unresolved source (point source) $A\delta(\xi_o,\eta_o)$ of strength A, at (ξ_o,η_o). The dirty image of this point source is $b_o(\xi,\eta)$ given by [18]

$$b_o(\xi,\eta) = \int\int \delta(\xi_o,\eta_o)P(\xi-\xi',\eta-\eta',\sqrt{1-\xi^2-\eta^2}-\sqrt{1-\xi'^2-\eta'^2})\mathrm{d}\xi\mathrm{d}\eta \tag{1.15}$$

which simplifies to

$$b_o(\xi,\eta) = AP(\xi_o-\xi',\eta_o-\eta',\sqrt{1-\xi_o^2-\eta_o^2}-\sqrt{1-\xi'^2-\eta'^2}) \tag{1.16}$$

The dirty image for a point source is called the dirty beam and is more commonly referred to as the synthesized beam or the point spread function (PSF).

We note from Equation 1.16 that it is not a function of the type $g(\xi_o-\xi)$ i.e., one of distance from the center and functionally depends on the term

$$\sqrt{1-\xi_o^2-\eta_o^2}-\sqrt{1-\xi'^2-\eta'^2}$$

Thus, the PSF will have different shapes depending on its position (ξ_o,η_o).

We write the brightness distribution measured with a non-coplanar array as:

$$\frac{A_N(\xi,\eta)B(\xi,\eta)}{\sqrt{1-\xi^2-\eta^2}} \star\star b_o(\xi,\eta) = \int\int\int W(x,y,z)V(x,y,z)e^{j2\pi\left(x\xi+y\eta+z\left(\sqrt{1-\xi^2-\eta^2}\right)\right)}\mathrm{d}x\mathrm{d}y\mathrm{d}z \tag{1.17}$$

where $b_o(\xi,\eta)$ is the synthesized beam and is a direct consequence of the visibilities being measured over a limited range of x, y, z, i.e., with some spectral sensitivity function $W(x, \mathrm{y}, \mathrm{x})$. $b_o(\xi,\eta)$ for a non-coplanar array varies with position (J,η).

The visibilities used in Equation 1.17 are generally obtained using an array of antennas with different interferometer spacings (baselines). The response of an interferometer to a non-varying radio source does not change from day to day and it follows that the information about the brightness distribution of the source can be derived from the elementary interferometer patterns taken one at a time. The sequential use of a set of baselines of an array of antennas to sample the visibilities is called aperture synthesis. Many aperture synthesis arrays also exploit the rotation of the earth to provide a continuous set of baselines. This is called earth-rotation synthesis.

In transforming the visibilities to brightness, it is convenient to use the Fast Fourier Transform (FFT) algorithm. This, however, requires the visibilities to be measured at regular intervals. In many arrays, the visibilities are not measured at regular intervals on the x, y plane. Hence, one cannot directly use the Fast Fourier Transform. In such a case, one can perform the transform using a Direct Fourier Transform which, however, takes longer time to process. Alternatively, one can 'grid' the measured visibilities onto a uniformly sampled plane and then apply the FFT. Gridding involves an interpolation of the available points and giving some value where no data points exist within a grid unit.

The transform in Equation 1.17 gives a 'dirty' map which is basically the convolution of the brightness distribution (modified by the antenna response function $A_N(\xi,\eta)$) with the synthesized beam, $b_o(\xi,\eta)$ (dirty-beam). A decon-

volution may then be performed to obtain an estimate of the true brightness distribution from the dirty-map. There are some established deconvolution techniques used such as CLEAN, invented by Hogbom [19]. This is the most widely used technique for deconvolution in radio astronomy. The Maximum Entropy Method (MEM) introduced in radio astronomy by Ables [20] is another widely used deconvolution technique.

For images obtained using non-coplanar arrays, the synthesized beam, $b_o(\xi, \eta)$, varies with the position of the source (ξ, η) and therefore the deconvolution needs to use different synthesized beams depending on the position of the source being deconvolved. Beam-sets [21] is one such technique wherein different synthesized beams are used for deconvolution depending on the position of the source. The declination shift algorithm [18] is another technique wherein the synthesized beam is generated for any declination, from the synthesized beam at a given declination. There are three-dimensional deconvolution techniques also [17], which operate on the 3-dimensional image volume $F(\xi, \eta, \zeta)$.

The Mauritius Radio Telescope (MRT) is similar to the classic T telescope [22] and has an east-west array of fixed antennas and a set of movable north-south antennas. However, the MRT is not coplanar. The visibilities are obtained by correlating the elements of the NS arm with those of the EW arm. A T array of dimensions $2L_{EW} \times L_{NS}$, gives the least redundant set of visibilities measurable with a rectangular aperture of dimensions $L_{EW} \times L_{NS}$[5]. At the MRT, $L_{EW} = 1024$ m and $L_{NS} = 880$ m. We discuss the antenna configuration, the receiver system and aspects of wide field imaging with the.

[5] A A arrangement, instead of a T, also gives the same information. The equivalent $\sqcap$ arrangement has arm lengths $L_{NS} \times L_{EW} \times L_{NS}$. Note: $T, \perp, \vdash, \dashv, \sqcap, \sqcup$ are all equivalent arrangements. The arrangement chosen could depend on terrain. In retrospect, a $\sqcap$ or a I-arrangement for the MRT could have helped avoid the highly non-coplanar western arm.

MRT in the following chapters.

However good the techniques of imaging may be, a telescope could be rendered ineffective by man-made interference. Hence it is important to protect frequency bands specifically for radio astronomy and develop ways of imaging to minimize the effects of interference. We discuss some aspects of the protection of radio frequencies for radio astronomy in the next section[6].

1.3 Protection of radio frequencies in astronomy

Radio astronomy does not involve transmission of radio waves and therefore cannot cause harmful interference to other services. The received cosmic signals are usually extremely weak, and transmissions from other services can interfere with such signals.

In radio astronomy, signals received from celestial sources have, in almost all cases, a Gaussian probability distribution in amplitude. Generally, it cannot be distinguished from thermal noise radiation of the Earth or its atmosphere, or from the noise generated in a receiver. The power contributed by the source under study is a factor of 10^{-2} to 10^{-6} lower than the unwanted power from the atmosphere, the ground and the receiver circuits. In communication systems, the corresponding signal-to-noise ratio is of the order of unity or greater. Furthermore the cosmic signals generally have no characteristic modulation that would help to distinguish them from noise. Another problem is the emission produced in the radio astronomy bands by active services operating in other bands. This is becoming more common as the use of broadband

[6] Much of the material presented on the protection of radio frequencies has been compiled from the *Handbook on Radio Astronomy, 1995* [23].

digital-modulation and spread-spectrum techniques continue to increase[7].

On the international scale, the regulation of spectrum usage is organized through the International Telecommunication Union (ITU), which is a specialized agency of the United Nations Organization. International frequency allocations are carried out at the World Radio Conferences (WRCs)[8] held every few years. For the purpose of allocation, the world is divided into three regions: Region 1 includes Europe, Africa and northern Asia; Region 2 includes North America and South America; Region 3 includes southern Asia and Australasia. The allocations are generally classified as primary or secondary allocations. A service with secondary allocation is not permitted to cause interference to a service with primary allocation in the same band. The frequency allocations are contained in Article 8 of the Radio Regulations. Although ground based observations are possible up to 1000 GHz, protection is provided only till 275 GHz in the Radio Regulations. Table 1.2 [23] gives a list of bands allocated to the radio astronomy service.

There are a large number of broadcast stations operating at both legal and illegal frequencies. Also there are a huge number of unlisted fixed and mobile transmitters. There is practically no band free below 12 MHz.

Most radio astronomy bands are shared with active services which transmit. Because of the great distances to astronomical sources, the power flux density levels of the sources under investigations are often 100 dB or more below those of man-made transmissions near the radio observatory. Interference can be damaging not only when it is strong and obliterates the astronomical signal

[7]For spectral lines in distant galaxies, an observed frequency that normally falls within a radio astronomy band may be Doppler shifted outside the band because of large motions of the galaxies relative to the earth. Therefore practically all parts of the radio spectrum are of potential scientific interest.

[8]WRCs were formerly known as World Administrative Radio Conferences (WARCs).

Frequency band (MHz)	Bandwidth (%)	Frequency band (GHz)	Bandwidth (%)
13.360 - 13.410	0.37	10.60 - 10.70	0.94
25.550 - 25.670	0.49	(14.47 - 14.50	(.21)
(37.5 - 38.25)	(1.98)	15.35 - 15.40	.33
73 - 74.6[1]	2.17	22.21 - 22.59	1.30
150.05 - 153[2]	1.95	23.6 - 24.0	1.68
322 - 328.6	2.03	31.3 - 31.8	1.58
406.1 - 410	0.96	42.5 - 43.5	2.33
608 - 614[3]	0.98	86 - 92	6.74
1400 - 1427	1.91	105 - 116	9.95
1660 - 1670	0.60	164 - 168	2.41
(2655 -2690)	(1.31)	182 - 185	1.63
2690 - 2700	0.37	217 - 231	6.25
(4800 - 4990)	(3.88)	265 - 275	3.70
4990 - 5000	0.20		

Table 1.2: Frequency bands allocated to the radio astronomy service. Secondary allocations are contained within brackets. (1) Primary Allocation in Region 2, protection recommended in Regions 1 and 3 (2.) Primary Allocation in Region 1, Australia and India (3) Primary Allocation in Region 2, China and India

but also when it is weak. Interference, which is say, just below the power level at which it can be recognized in individual measurements and which is present for a large fraction of time, could cause serious errors in the images of astronomical sources.

The criteria for protection in radio astronomy include:

a) The power level of the interference considered harmful.

b) The fraction of the sky over which radio astronomy observations are to be protected.

c) The fraction of time over which the observations are protected.

The above criteria are directly related to geographical sharing of the two services, i.e., the geographical spacing of two services which enable both to work at the same frequency at the same time. In sharing between services, ad-

ditional protection may be obtained by use of orthogonal polarizations. This is not a very useful technique since interference generally enters through sidelobes with polarization characteristics very different from that of the main beam. Also, many radio observations require observations with both polarizations. It should be noted that generally sharing frequency with the radio astronomy service is possible only when there is considerable geographical separation. Limited time-sharing to permit special observations at a radio astronomy site may be possible, and may indeed be necessary.

The radio astronomy bands occupy only about 2% of the radio spectrum below 50 GHz. Protection of these bands is mandatory to continue observations in the future. These bands will also allow passive remote sensing of the earth's environment and natural resources from outer space.

A totally interference-free site may be a thing of the past, specially at low frequencies. It is therefore imperative for the radio astronomy community to develop techniques to minimize the effect of interference. In Mauritius the band around 150 MHz is not a primary allocation for radio astronomy. The Government of Mauritius has allocated a 1 MHz band from 150 MHz to 151 MHz for radio astronomy. However, there is a communication facility operating at 149 MHz, emission from which spills into this protected band making it unusable. There is also interference from unidentified satellite(s) in this band. We have therefore moved the frequency of operation from the initially planned observing frequency of 150 MHz to 151.5 MHz. A narrow band around 151.5 MHz is relatively free of interference. Since this is not a protected band in Mauritius, an application for protection of this frequency has been made to the Government of Mauritius. We have also developed techniques to detect interference in the visibility data and overcome the effects

of interference in the final images. These are discussed in Chapter **4.** We also give statistics of the interference in the observations made at the MRT.

1.4 Thesis layout

The thesis comprises of six chapters. The layout of the remaining chapters are summarized below

- Chapter **2** describes the Mauritius Radio Telescope. Details of the array layout, the front-end, and the receiver system employed are given.
- Chapter **3** describes the problems of wide field imaging with the MRT and the need for a hardware system (recirculator) to efficiently image a large field of view. The design aspects along with a description of the hardware systems developed and the observations made with them are given.
- Chapter **4** describes various aspects of data analysis for wide field imaging with the MRT using the recirculator system. Calibration and imaging of the recirculator data for wide fields are discussed. As part of the data analysis interference detection and their excision are also discussed.
- Chapter **5** discusses the various results obtained. A one hour region has been imaged at **151.5** MHz with a resolution of $4' \times 9'.12 \sec(\delta + 20°.14)$ covering the entire declination range of the MRT, $-70° \leq \delta \leq -10°$. Sensitivity and estimation of the positions and flux densities of unresolved sources in the image are also discussed.
- Chapter 6 summarizes the work presented. Conclusions and a few suggestions for future work are also presented.